Catalytic effect of CeCl$_3$ on the hydrogen storage properties of MgH$_2$

M. Ismail*, N.S. Mustafa, N. Juahir, F.A. Halim Yap

School of Ocean Engineering, Universiti Malaysia Terengganu, 21030 Kuala Terengganu, Malaysia

HIGHLIGHTS

- Hydrogen storage properties of CeCl$_3$-doped MgH$_2$ prepared by ball milling were investigated.
- Adding with CeCl$_3$ reduced the decomposition temperature and enhanced the sorption kinetics of MgH$_2$.
- The *in-situ* formation of Ce–Mg alloy, CeH$_{2.73}$, and MgCl$_2$ may play an important role.

ARTICLE INFO

ABSTRACT

The effects of CeCl$_3$ addition on the hydrogen storage properties of MgH$_2$ prepared by ball milling were investigated for the first time. The 10 wt.% CeCl$_3$-added MgH$_2$ sample showed an improvement in hydrogenation sorption properties compared to that of undoped MgH$_2$, with the onset dehydrogenation temperature reduced from 350 °C to 300 °C. Kinetic desorption results showed that CeCl$_3$-added MgH$_2$ released about 5.5 wt.% hydrogen within 10 min at 350 °C, while the as-milled MgH$_2$ released below 3.1 wt.% hydrogen within the same time period and temperature. Meanwhile, hydrogen absorption capacity of 5.2 wt.% was reached at 280 °C in 5 min for the CeCl$_3$-doped MgH$_2$ sample. In contrast, the ball-milled MgH$_2$ only absorbed 4.0 wt.% hydrogen at 280 °C in 5 min. From the Kissinger plot of differential scanning calorimetry, the apparent activation energy was 167.0 kJ/mol for as-milled MgH$_2$ and 149.0 kJ/mol for 10 wt.% CeCl$_3$-added MgH$_2$, indicating that CeCl$_3$ addition decreased the activation energy for hydrogen desorption of MgH$_2$. The improved hydrogen storage properties of MgH$_2$ in the presence of CeCl$_3$ are believed to be due to the role of *in situ* formed Ce–Mg alloy, MgCl$_2$, and CeH$_{2.73}$ as active species to catalyse the hydrogen storage properties of MgH$_2$.

1. Introduction

MgH$_2$ is an attractive potential for solid-state hydrogen storage material because it has high gravimetric capacity of 7.6 wt.%, low cost, and superior reversibility. However, high thermodynamic stability ($\Delta H \sim -75$ kJ/mol H$_2$) and the slow kinetics of hydride formation and decomposition render the use of MgH$_2$ for practical purposes. Many studies have been done to improve the thermodynamic property and kinetics behaviour of MgH$_2$ through using mechanical milling both with and without catalytic additives. The effects of ball-milling pure MgH$_2$ have been studied since the late 1990s [1,2], although the temperatures required for decomposition were still too high for practical applications. Meanwhile, catalyst investigation plays a crucial role in the development of solid-state

hydrogen storage based on MgH$_2$. Previous studies have shown that by using several catalysts and additives, thermodynamic property and de/rehydrogenation kinetic parameters of MgH$_2$ could be improved. In these studies, metal [3,4], metal oxide [5], metal halides [6–11], metal hydride [12], carbon materials [13], nanosized alloys [4,14–18], and combination carbon with other materials [19–21] were used as the catalysts and additives. Among the catalysts used above, metal halide was found to be the most promising catalyst. Although the addition of metal halides on MgH$_2$ improves the performance, a complete understanding of the roles play by catalysts is still an open issue and further investigations are highly desired.

Another halides family, rare-earth chlorides, has been widely applied as a catalyst in light complex metal hydrides, such as NaAlH$_4$ [22–28] and LiAlH$_4$ [29,30]. However, the effect of rare-earth chlorides as a catalyst for hydrogen storage properties of MgH$_2$ has not been explored as thoroughly as NaAlH$_4$ and LiAlH$_4$. To the best of the authors' knowledge, until now, only one kind of rare-

* Corresponding author.
  E-mail address: mohammadismail@umt.edu.my (M. Ismail).

earth chloride ($LaCl_3$) has been reported as the catalyst for the development of hydrogen storage performance of MgH_2, as reported in the authors' previous study [31]. So, it is interesting to examine other rare-earth chlorides as a catalyst or additive for hydrogen storage properties of MgH_2.

Recently, a study by Fan et al. [26] has shown that the hydrogen storage properties of $NaAlH_4$ have been improved with the addition of $CeCl_3$. They claimed that the *in situ* formed $CeAl_4$ acted as active species to catalyse the reversible dehydrogenation and rehydrogenation of $NaAlH_4$. More recently, Hu et al. [25] have reported that the introduction of $CeCl_3$ into $NaAlH_4$ was also effective in enhancing the sorption kinetics of $NaAlH_4$. They suggested that $CeCl_3$ was readily converted by ball-milling in the presence of $NaAlH_4$ to cerium hydride which further formed cerium aluminides ($CeAl_x$) in the cycling process. Although both cerium hydride and $CeAl_x$ showed catalytic effect in the kinetics enhancement, $CeAl_x$ was found to be more effective than its counterpart, cerium hydride. Both of the articles above speculated that the *in situ* formed Ce–Al acted as active species and further improved the hydrogen storage properties of $NaAlH_4$. Therefore, it is reasonable to believe that $CeCl_3$ has a great potential as a catalyst to improve the hydrogen storage properties of MgH_2 through positive factors of *in situ* active species.

In the present work, with the aim of *in situ* active species role, the catalytic effects of adding $CeCl_3$ as a catalyst precursor on the de/rehydrogenation behaviour of MgH_2 are investigated. The possible mechanism is discussed based on the experimental results.

2. Experimental details

MgH_2 powder (hydrogen-storage grade) was purchased from Sigma–Aldrich and $CeCl_3$ powder (anhydrous, 99.5% (REO)) was purchased from Alfa Aesar. All the compounds were used as-received with no further purification. Handling of the samples was performed in an MBraun Unilab glove box filled with high-purity Ar atmosphere. Doping was implemented by ball-milling. About 400 mg of MgH_2 was mixed with 10 wt.% $CeCl_3$. Each sample was put into a sealed stainless steel vial together with hardened stainless steel balls. Ball milling was performed in a planetary ball mill (NQM-0.4) for 1 h by milling for 0.5 h, resting for 6 min, and then continued milling for another 0.5 h in a different direction at a rate of 400 rpm. A fan was used as the air-cooling system for the vial to prevent overheating during the ball milling process.

Experiments for de/re-hydrogenation were performed in a Sieverts-type pressure-composition-temperature (PCT) apparatus (Advanced Materials Corporation). About 100 mg of the sample was loaded into a sample vessel for each test. For desorption purposes, all of the samples were heated in a vacuum chamber, and the amount of desorbed hydrogen was measured to determine the lowest decomposition temperature. The heating rate for desorption experiment was 5 °C/min, and the samples were heated from room temperature to 450 °C under vacuum. The de/rehydrogenation kinetics measurements were conducted at the desired temperature with initial hydrogen pressures of 0.1 atm and 30 atm, respectively.

The phase structures for the as-milled samples, after desorption, and after rehydrogenation, were determined by Rigaku MiniFlex X-ray diffractometer with Cu Ka radiation. Before the measurement, a small amount of sample was spread uniformly on the sample holder and wrapped with a plastic wrap to prevent oxidation. The X-ray intensity was measured over diffraction angles from 20° to 80° with a scanning rate of 2.00°/min.

Differential scanning calorimetry (DSC) analysis of the as-prepared powder samples was carried out using a Mettler Toledo TGA/DSC 1. About 2–6 mg of the sample was loaded into an alumina crucible in the glove box. Subsequently, the crucible was placed in a sealed glass bottle in order to prevent oxidation during the transfer from the glove box to the DSC apparatus. An empty alumina crucible was used for reference. The samples were heated from room temperature until 500 °C under Ar atmosphere, and different heating degrees were used.

3. Results and discussion

Fig. 1 shows the temperature-programmed desorption (TPD) patterns for dehydrogenation of as-received MgH_2, as-milled MgH_2, and MgH_2 + 10 wt.% $CeCl_3$. The as-received MgH_2 started to release hydrogen at approximately 410 °C, with a total dehydrogenation capacity of about 7.0 wt.% H_2 by 430 °C. After milling, the onset desorption temperature of MgH_2 was reduced to about 350 °C, indicating that the milling process also influenced the onset desorption temperature of MgH_2, as reported in the literature [1]. After doping with $CeCl_3$, the onset desorption temperature of MgH_2 decreased dramatically. The doped sample started to release hydrogen at about 300 °C, a decrease of about 50 °C and 110 °C, compared to the as-milled and as-received MgH_2, respectively.

Further studies concerning the catalytic activity of $CeCl_3$ on the dehydrogenation of MgH_2 were carried out by evaluating the desorption kinetics. In order to determine the dehydrogenation kinetic of MgH_2 + 10 wt.% $CeCl_3$ composite, isothermal dehydrogenation was studied at 350 °C, as shown in Fig. 2. The dehydrogenations of undoped MgH_2 were also included for comparison under the same condition. The result showed that undoped MgH_2 released about 3.0 wt.% of hydrogen after 10 min. Meanwhile, the dehydrogenated MgH_2 + 10 wt.% $CeCl_3$ composite showed faster desorption than the undoped MgH_2. Saturation of the dehydrogenation process for $CeCl_3$-doped MgH_2 sample can be achieved within 10 min with about 5.5 wt.% of hydrogen release. Comparing the results, it can be seen that $CeCl_3$ also played an important role in improving the dehydrogenation kinetic of MgH_2.

For further investigation on hydrogen absorption kinetics, the quantity of hydrogen absorbed from doped and undoped samples at constant temperature was measured. Fig. 3 shows the hydrogenation kinetics of milled MgH_2 and MgH_2 + 10 wt.% $CeCl_3$ composite at 280 °C under 30 atm H_2. Obviously, MgH_2 + 10 wt.% $CeCl_3$ composite has better hydrogenation kinetics than undoped MgH_2. MgH_2 + 10 wt.% $CeCl_3$ composite can absorb about 5.6 wt.% hydrogen at 280 °C in 10 min under 30 atm H_2. In contrast, the

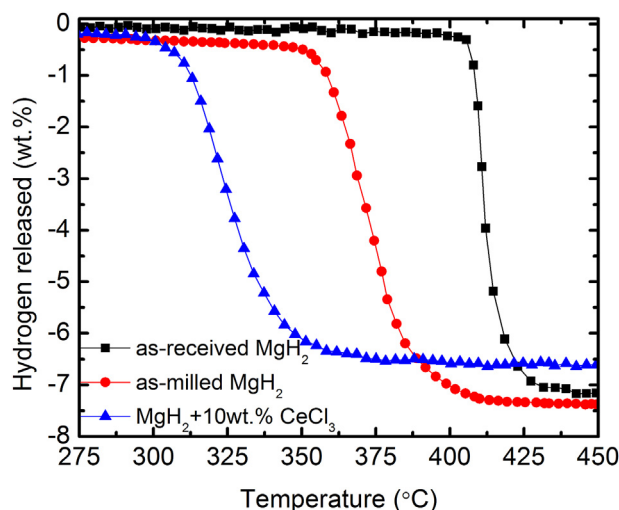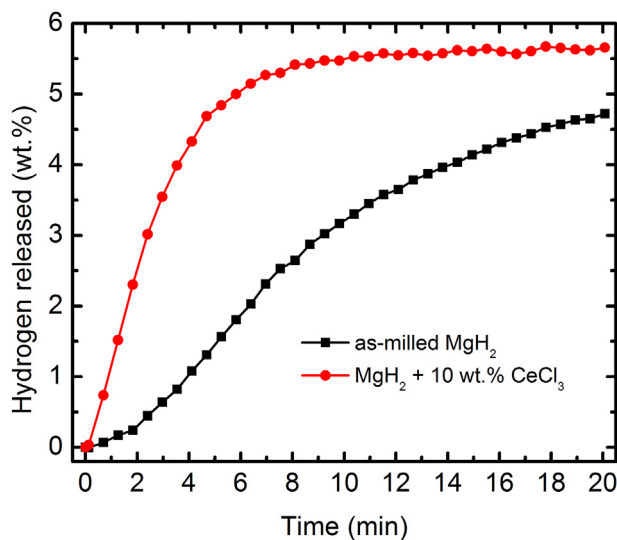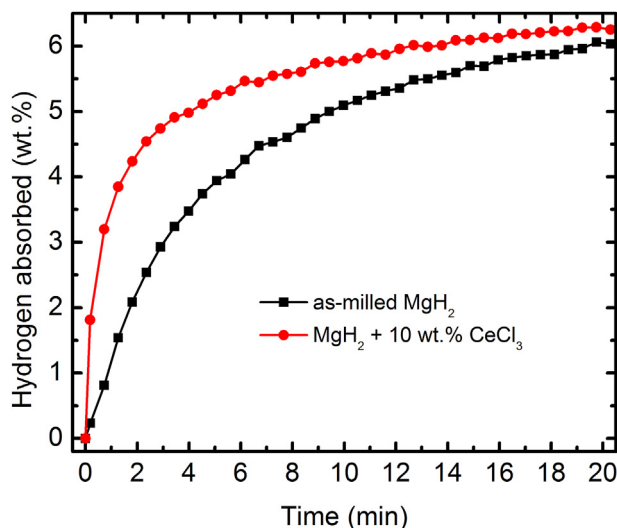**Fig. 1.** Temperature-programmed desorption (TPD) patterns for the dehydrogenation of as-received MgH_2, as-milled MgH_2, and MgH_2 doped with 10 wt.% $CeCl_3$.

Fig. 2. Isothermal desorption kinetics curves for as-milled MgH_2 and MgH_2 doped with 10 wt.% $CeCl_3$ at 350 °C under vacuum.

Fig. 3. Isothermal absorption kinetics measurement of as-milled MgH_2 and MgH_2 doped with 10 wt.% $CeCl_3$ at 280 °C under 30 atm hydrogen pressure.

undoped MgH_2 can only absorb about 5.0 wt.% hydrogen in the same condition. The results clearly suggest that the addition of $CeCl_3$ is responsible for hydrogenation kinetic enhancement.

Thermal properties of the as-milled MgH_2 and $CeCl_3$-doped MgH_2 samples were further investigated by DSC, as shown in Fig. 4. The as-milled MgH_2 started to release hydrogen at about 370 °C. After doping with $CeCl_3$, MgH_2 started to release hydrogen at about 320 °C, which represents a reduction of about 50 °C compared to as-milled MgH_2. This result is comparable with the results of PCT measurements (Fig. 1). Furthermore, it can be seen that the onset decomposition temperatures of the samples in DSC were slightly higher than in the TPD (Fig. 1). These differences may result from the fact that dehydrogenation was conducted under different heating rates and atmospheres in two types of measurements. The DSC measurement was run under 1 atm argon flow with a heating rate of 10 °C/min; while the TPD measurement was conducted under the condition of 0.1 atm vacuum with 5 °C/min heating rate, resulting different driving forces during the desorption process
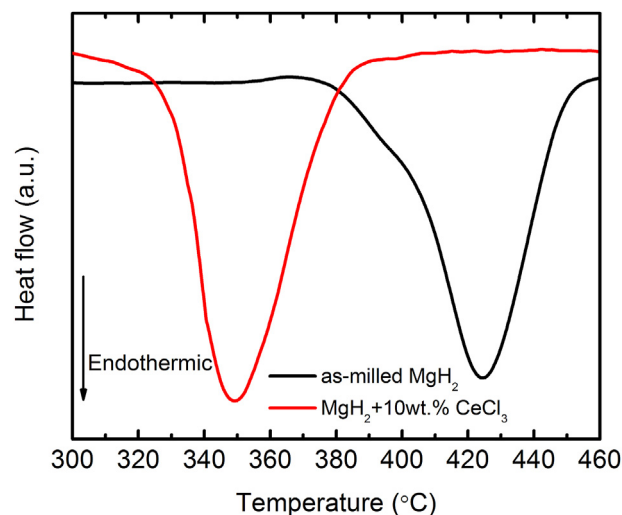
Fig. 4. DSC traces of as-milled MgH_2 and $MgH_2 + 10$ wt.% $CeCl_3$. Heating rate: 10 °C/min, argon flow: 30 ml/min.

[32]. A similar phenomenon has also appeared in our previous papers [33–37].

In order to determine the hydrogen desorption enthalpy (ΔH_{dec}) of MgH_2 decomposition, the DSC curves were analysed by STARe software and the hydrogen desorption enthalpy was obtained from the integrated peak areas. The hydrogen desorption enthalpy for as-milled MgH_2 was calculated as 75.7 kJ/mol H_2, which is almost the same as the theoretical value (76 kJ/molH_2). After the addition of $CeCl_3$, the enthalpy of hydrogen desorption of MgH_2 was similar to that of undoped MgH_2. These results indicate that the additive investigated in this work acted as a catalyst and did not change the thermodynamics of the system. This phenomenon is similar to a report by Malka et al. on ZrF_4, NbF_5, TaF_5, and $TiCl_3$ doped MgH_2 [10]. However, other studies have reported that both thermodynamic and kinetics properties could be adjusted at the same time with the addition of metals such as In, Al, Ti, and Ni [38–40].

The improvement of dehydrogenation properties is related to the energy barrier of H_2 released from MgH_2. In the present study, the activation energy for decomposition of MgH_2 was reduced by adding $CeCl_3$. To calculate the activation energy of as-milled MgH_2 and $CeCl_3$-added MgH_2, the Kissinger plot was used. The plot was obtained based on the Kissinger equation [41] as follows:

$$\ln[\beta/T_p^2] = -E_A/RT_p + A \tag{1}$$

where β is the heating rate, T_p is the peak temperature in the DSC curve, E_A is the activation energy, R is the molar gas constant (8.3144621 J/(mol K)), and A is a constant. Thus, the activation energy, E_A, can be obtained from the slope by plotting a graph of ln $[\beta/T^2_p]$ versus $1000/T_p$. Fig. 5(a) and Fig. 5(b) show the DSC traces of as-milled MgH_2 and $CeCl_3$-doped MgH_2 samples, respectively, at different heating rates. Based on the Kissinger plot of DSC data, as shown in Fig. 6, the activation energy for as-milled MgH_2 obtained was 167.0 kJ/mol. Meanwhile, the apparent activation energy for decomposition of $CeCl_3$-doped MgH_2 composite was found to be 149.0 kJ/mol, significantly lower compared to as-milled MgH_2. This indicates that $CeCl_3$ additive also played an important role in reducing the activation energy of H-desorption in MgH_2.

The SEM images of as-received and as-milled MgH_2 and $MgH_2 + 10$ wt.% $CeCl_3$ are shown in Fig. 7. For as-received MgH_2 (Fig. 7)(a), it is evident that majority of the MgH_2 particles have an angular shape with an average size of approximately larger than
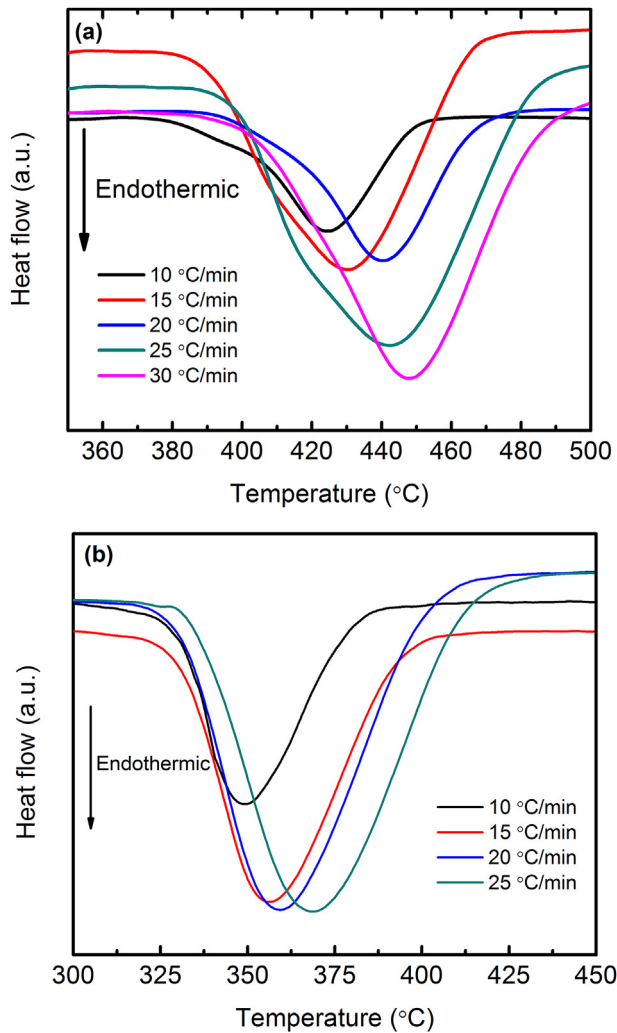
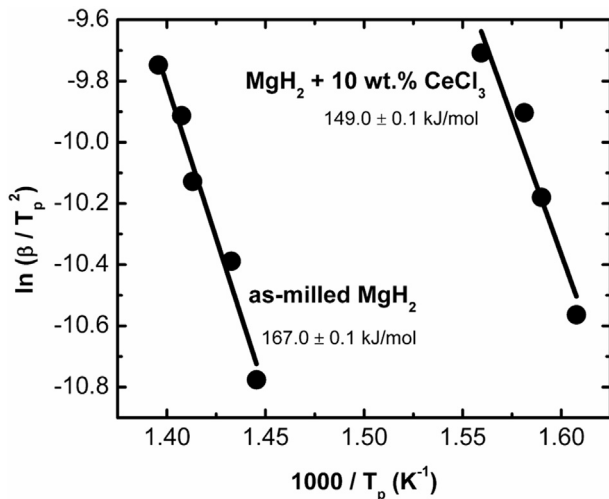**Fig. 5.** DSC traces at different heating rates for (a) as-milled MgH$_2$ and (b) MgH$_2$ + 10 wt.% CeCl$_3$.

Fig. 6. The Kissinger's plot of dehydrogenation for 10 wt.% CeCl$_3$-doped MgH$_2$ composite as compared with as-milled MgH$_2$.

100 μm. After ball milling (Fig. 7)(b), the powders changed to nearly spherical shape and agglomerated. The size of as-milled MgH$_2$ powders reduced drastically. Meanwhile, as shown in Fig. 7(c), the size of CeCl$_3$-doped MgH$_2$ particles was smaller than that of as-milled MgH$_2$. This is probably due to the hardness of the CeCl$_3$ which would have help breaking the MgH$_2$ particles into smaller sizes. It is already well-known that as the surface area of contact increases, the rate of reaction for MgH$_2$ to release and absorb H$_2$ will also increase. In addition, smaller particle size will improve hydrogen absorption/desorption because it reduces the diffusion length of the hydrogen and makes the particles' reactive surface larger [18]. So, from the morphology results, it is speculated that the hydrogen storage properties of MgH$_2$ + 10 wt.% CeCl$_3$ sample were improved as a result of the reduced particle size.

In order to clarify the phase structure of CeCl$_3$-doped MgH$_2$ sample after 1 h milling, after dehydrogenation at 450 °C, and after rehydrogenation at 280 °C under 30 atm hydrogen pressure, XRD was used, as shown in Fig. 8. After ball milling processes (Fig. 8)(a), the main phases presented were the formations of parent materials, MgH$_2$ and CeCl$_3$. No new compounds were formed from the mixtures. After dehydrogenation at 450 °C, XRD pattern (Fig. 8)(b) revealed that there were distinct peaks of Mg, which indicate that the dehydrogenation process of MgH$_2$ was completed. In addition, the peaks for CeCl$_3$ disappeared, and some new peaks corresponding to Ce–Mg alloy (MgCe) (crystallizes in cubic space group *Pm3m* with the lattice parameters of a = 3.899 Å and z = 1 Å, as identified using the powder diffraction file (PDF) 18–318) and MgCl$_2$ were observed, suggesting that the reaction of MgH$_2$ with CeCl$_3$ may occur during the heating process, as follows:

$$5MgH_2 + 2CeCl_3 \rightarrow 3MgCl_2 + 2MgCe + 5H_2 \qquad (2)$$
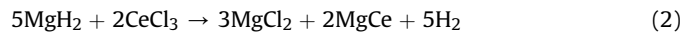
In the XRD pattern of rehydrogenated sample (Fig. 8)(c), characteristic diffraction peaks of Mg disappeared, while characteristic diffraction peaks of MgH$_2$ appeared, indicating that Mg was largely transformed into MgH$_2$ during the rehydrogenation process. After rehydrogenation, the Ce–Mg alloy peaks disappeared, and the peaks of CeH$_{2.73}$ (crystallizes in cubic space group *Fm-3m* with the lattice parameters of a = 5.53000 Å and z = 4 Å, as identified using the powder diffraction file (PDF) 89–3694) appeared, indicating that Ce–Mg alloy can be dissociated into CeH$_{2.73}$ and MgH$_2$ as reported by Ouyang et al. [42]. The disproportionation reaction in hydrogenation process of Mg-RE-alloys system has been widely reported previously [43–46]. In addition, MgCl$_2$ peak remained unchanged after the rehydrogenation process.

From the experimental results, improved hydrogen storage properties of MgH$_2$ by doping with CeCl$_3$ could be speculated by several factors. The formation of Ce–Mg alloy and CeH$_{2.73}$ during dehydrogenation and rehydrogenation process may play an important role in the enhancement of MgH$_2$ sorption. It is well-known that dehydrogenation products in light metal hydride catalyst system could act as a real catalyst to facilitate the dehydrogenation step. These products could create surface activation and form a large number of nucleation sites at the surface of MgH$_2$ matrix [47,48]. In addition, many findings have exposed the catalytic effect of *in situ* formed rare hydrides on rehydrogenation process of MgH$_2$. In this study, CeH$_{2.73}$ may act as H diffusion channels and nucleation sites of hydrides as reported by Ouyang et al. [42] for Mg$_{80}$Ce$_{18}$Ni$_2$ composite system. Moreover, Cl$^-$ may also introduce an extra catalytic effect on MgH$_2$ sorption properties. As discussed in the literature [10,49], the catalytic effect of metal halides on hydrogen sorption of MgH$_2$ could also be simultaneously influenced by a number of reasons such as formation of MgF$_2$ and catalytic influence of transition metal halides (with different levels of metal oxidation state). Based on these, in this study, the chlorine-
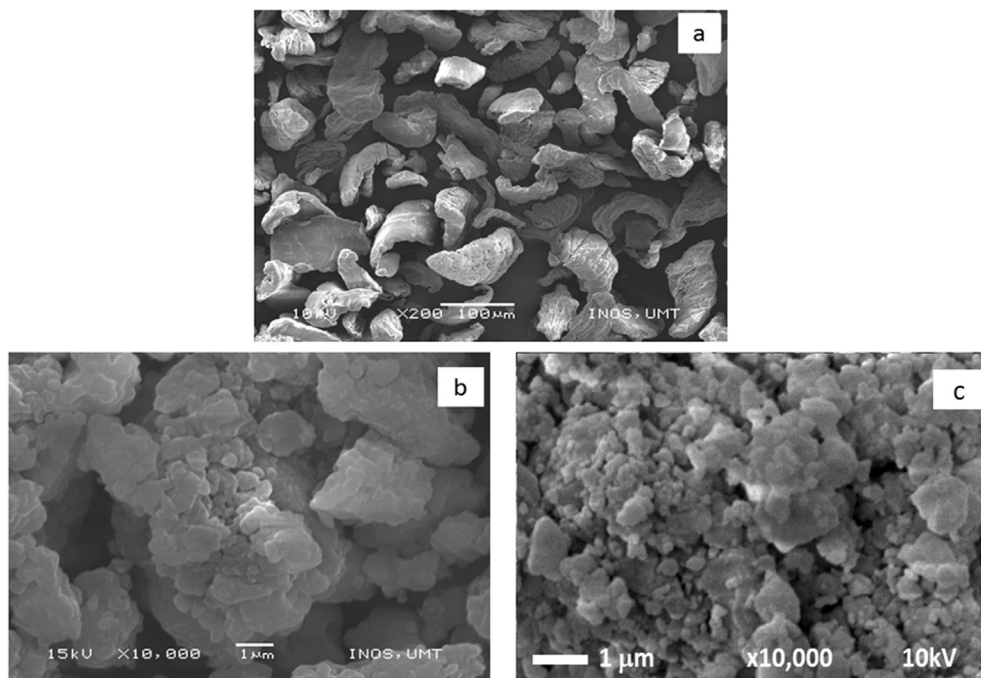
Fig. 7. SEM images of (a) as-received MgH_2, (b) as-milled MgH_2 and (c) MgH_2 + 10 wt% $CeCl_3$.

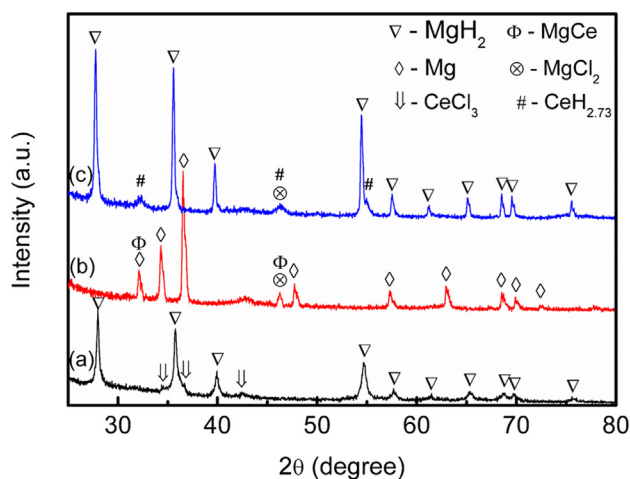**Fig. 8.** X-ray diffraction patterns of 10 wt.% $CeCl_3$-doped MgH_2 (a) after milling, (b) after dehydrogenation, and (c) after rehydrogenation.

based product, $MgCl_2$, may also introduce an extra catalytic effect on MgH_2 sorption properties, as proved in previous reports [6,50]. Catalytic effect of $MgCl_2$ may further combine with the catalytic function of Ce–Mg alloy and $CeH_{2.73}$ species to generate a synergetic effect. Besides, the addition of metal halides may also result in the generation of diffusion paths that would affect the kinetics of MgH_2 hydrogenation. Further investigation is required to clarify the exact role of $CeCl_3$ additive on the enhancement of hydrogen storage properties of MgH_2 such as investigating the effect of different amount of $CeCl_3$ and by observation methods such as transmission electron microscopy.

4. Conclusion

In summary, we have demonstrated that adding a small amount of $CeCl_3$ powder by dry ball milling reduced the decomposition temperature and enhanced the sorption kinetics of MgH_2. Adding 10 wt.% $CeCl_3$ reduced the decomposition temperature of MgH_2 by 50 °C compared to as-milled MgH_2. The added material started to release hydrogen at about 300 °C, and dehydrogenation was completed below 375 °C with approximately 6.50 wt.% of H_2 release. Furthermore, kinetic desorption results showed that the addition of MgH_2 released about 5.5 wt.% hydrogen within 10 min at 350 °C, while as-milled MgH_2 only released about 3.1 wt.% hydrogen within the same time period. Meanwhile, about 5.2 wt.% hydrogen was absorbed at 280 °C under 30 atm hydrogen in 5 min for $CeCl_3$-doped MgH_2 sample, while MgH_2 sample only absorbed about 4.0 wt.% hydrogen under the same conditions. This indicates that the $CeCl_3$-added sample has shown a significant improvement in de/rehydrogenation rates compared to that of as-received MgH_2. From the Kissinger plot of differential scanning calorimetry, apparent activation energy was 149 kJ/mol for $CeCl_3$-added MgH_2 and 167 kJ/mol for MgH_2. Adding 10 wt.% $CeCl_3$ reduced the activation energy of MgH_2, thus promoting decomposition at a lower temperature. It is believed that the significant effect of $CeCl_3$ addition on dehydrogenation behaviour of MgH_2 is attributable to the catalytic activity of the *in situ* formed Ce–Mg alloy, $CeH_{2.73}$, and $MgCl_2$ as active species. From the experimental results, it can be concluded that $CeCl_3$ is an excellent additive for dehydrogenation of MgH_2.

References

[1] J. Huot, G. Liang, S. Boily, A. Van Neste, R. Schulz, J. Alloys Compd. 293–295 (1999) 495–500.
[2] A. Zaluska, L. Zaluski, J.O. Ström-Olsen, J. Alloys Compd. 288 (1999) 217–225.
[3] N. Hanada, T. Ichikawa, H. Fujii, J. Phys. Chem. B 109 (2005) 7188–7194.
[4] S.F. Santos, T.T. Ishikawa, W.J. Botta, J. Huot, Mater. Chem. Phys. 147 (2014) 557–562.
[5] J. Shan, P. Li, Q. Wan, F. Zhai, J. Zhang, Z. Li, Z. Liu, A.A. Volinsky, X. Qu, J. Power Sources 268 (2014) 778–786.
[6] M. Ismail, Int. J. Hydrogen Energy 39 (2014) 2567–2574.
[7] F.A. Halim Yap, N.S. Mustafa, M. Ismail, RSC Adv. 5 (2015) 9255–9260.
[8] L.P. Ma, X.D. Kang, H.B. Dai, Y. Liang, Z.Z. Fang, P.J. Wang, P. Wang, H.M. Cheng, Acta Mater. 57 (2009) 2250–2258.
[9] N.S. Mustafa, M. Ismail, Int. J. Hydrogen Energy 39 (2014) 15563–15569.
[10] I.E. Malka, M. Pisarek, T. Czujko, J. Bystrzycki, Int. J. Hydrogen Energy 36 (2011) 12909–12917.
[11] M. Ismail, Y. Zhao, X.B. Yu, S.X. Dou, Energy Edu. Sci. Technol. Part A Energy Sci. Res. 30 (2012) 107–122.
[12] J. Lu, Y.J. Choi, Z.Z. Fang, H.Y. Sohn, E. Ronnebro, J. Am. Chem. Soc. 131 (2009) 15843–15852.
[13] C.X. Shang, Z.X. Guo, J. Power Sources 129 (2004) 73–80.
[14] X.B. Yu, Z.X. Yang, H.K. Liu, D.M. Grant, G.S. Walker, Int. J. Hydrogen Energy 35 (2010) 6338–6344.
[15] X.B. Yu, Y.H. Guo, Z.X. Yang, Z.P. Guo, H.K. Liu, S.X. Dou, Scr. Mater. 61 (2009) 469–472.
[16] X.B. Yu, Y.H. Guo, H. Yang, Z. Wu, D.M. Grant, G.S. Walker, J. Phys. Chem. C 113 (2009) 5324–5328.
[17] A. Ranjbar, Z.P. Guo, X.B. Yu, D. Attard, A. Calka, H.K. Liu, Int. J. Hydrogen Energy 34 (2009) 7263–7268.
[18] A. Ranjbar, Z.P. Guo, X.B. Yu, D. Wexler, A. Calka, C.J. Kim, H.K. Liu, Mater. Chem. Phys. 114 (2009) 168–172.
[19] X. Yao, C. Wu, A. Du, J. Zou, Z. Zhu, P. Wang, H. Cheng, S. Smith, G. Lu, J. Am. Chem. Soc. 129 (2007) 15650–15654.
[20] M. Ismail, N. Juahir, N.S. Mustafa, J. Phys. Chem. C 118 (2014) 18878–18883.
[21] A. Ranjbar, M. Ismail, Z.P. Guo, X.B. Yu, H.K. Liu, Int. J. Hydrogen Energy 35 (2010) 7821–7826.
[22] B. Bogdanovic, M. Felderhoff, A. Pommerin, F. Schueth, N. Spielkamp, Adv. Mater. 18 (2006) 1198–1201.
[23] T. Sun, B. Zhou, H. Wang, M. Zhu, Int. J. Hydrogen Energy 33 (2008) 2260–2267.
[24] Z. Xueping, L. Shenglin, L. Donglin, Int. J. Hydrogen Energy 34 (2009) 2701–2704.
[25] J. Hu, S. Ren, R. Witter, M. Fichtner, Adv. Energy Mater. 2 (2012) 560–568.
[26] X. Fan, X. Xiao, L. Chen, S. Li, Q. Wang, J. Alloys Compd. 509 (Suppl. 2) (2011) S750–S753.
[27] X. Fan, X. Xiao, L. Chen, L. Han, S. Li, H. Ge, Q. Wang, Int. J. Hydrogen Energy 36 (2011) 10861–10869.
[28] X. Fan, X. Xiao, L. Chen, K. Yu, Z. Wu, S. Li, Q. Wang, Chem. Commun. (2009) 6857–6859.
[29] Z. Xueping, L. Ping, I.S. Humail, A. Fuqiang, W. Guoqing, Q. Xuanhui, Int. J. Hydrogen Energy 32 (2007) 4957–4960.
[30] Z. Xueping, L. Shenglin, J. Alloys Compd. 481 (2009) 761–763.
[31] M. Ismail, Energy 79 (2015) 177–182.
[32] F. Zhai, P. Li, A. Sun, S. Wu, Q. Wan, W. Zhang, Y. Li, L. Cui, X. Qu, J. Phys. Chem. C 116 (2012) 11939–11945.
[33] M. Ismail, Y. Zhao, X.B. Yu, S.X. Dou, Int. J. Hydrogen Energy 35 (2010) 2361–2367.
[34] M. Ismail, Y. Zhao, X.B. Yu, A. Ranjbar, S.X. Dou, Int. J. Hydrogen Energy 36 (2011) 3593–3599.
[35] M. Ismail, Y. Zhao, X.B. Yu, I.P. Nevirkovets, S.X. Dou, Int. J. Hydrogen Energy 36 (2011) 8327–8334.
[36] M. Ismail, Y. Zhao, X.B. Yu, S.X. Dou, Int. J. Electroactive Mater. 1 (2013) 13–22.
[37] M. Ismail, A. Sinin, C. Sheng, W.W. Nik, Int. J. Electrochem. Sci. 9 (2014) 4959–4973.
[38] Z. Cao, L. Ouyang, Y. Wu, H. Wang, J. Liu, F. Fang, D. Sun, Q. Zhang, M. Zhu, J. Alloys Compd. 623 (2015) 354–358.
[39] L.Z. Ouyang, Z.J. Cao, H. Wang, J.W. Liu, D.L. Sun, Q.A. Zhang, M. Zhu, Int. J. Hydrogen Energy 38 (2013) 8881–8887.
[40] L.Z. Ouyang, Z.J. Cao, H. Wang, J.W. Liu, D.L. Sun, Q.A. Zhang, M. Zhu, J. Alloys Compd. 586 (2014) 113–117.
[41] H.E. Kissinger, Anal. Chem. 29 (1957) 1702–1706.
[42] L.Z. Ouyang, X.S. Yang, M. Zhu, J.W. Liu, H.W. Dong, D.L. Sun, J. Zou, X.D. Yao, J. Phys, Chem. C 118 (2014) 7808–7820.
[43] L.Z. Ouyang, F.X. Qin, M. Zhu, Scripta Mater. 55 (2006) 1075–1078.
[44] L.Z. Ouyang, H.W. Dong, C.H. Peng, L.X. Sun, M. Zhu, Int. J. Hydrogen Energy 32 (2007) 3929–3935.
[45] L.Z. Ouyang, X.S. Yang, H.W. Dong, M. Zhu, Scripta Mater. 61 (2009) 339–342.
[46] L.Z. Ouyang, Y.J. Xu, H.W. Dong, L.X. Sun, M. Zhu, Int. J. Hydrogen Energy 34 (2009) 9671–9676.
[47] P. Li, Q. Wan, Z. Li, F. Zhai, Y. Li, L. Cui, X. Qu, A.A. Volinsky, J. Power Sources 239 (2013) 201–206.
[48] F. Zhai, P. Li, A. Sun, S. Wu, Q. Wan, W. Zhang, Y. Li, L. Cui, X. Qu, J. Phys. Chem. C 116 (2012) 11939–11945.
[49] I.E. Malka, T. Czujko, J. Bystrzycki, Int. J. Hydrogen Energy 35 (2010) 1706–1712.
[50] J. Mao, Z. Guo, X. Yu, H. Liu, Z. Wu, J. Ni, Int. J. Hydrogen Energy 35 (2010) 4569–4575.